Static fatigue of multifilament tows at high temperatures above 900°C

Adrien Laforêt, Jacques Lamon

University of Bordeaux/CNRS
Laboratoire des Composites Thermostructuraux
3 Allée de La Boétie
33600 Pessac, France
lamon@lcts.u-bordeaux1.fr

ABSTRACT

Previous work has shown that SiC-based fibers are sensitive to delayed failure at temperatures below 800°C. This behaviour has been attributed to slow crack growth driven by oxidation of carbon grain boundaries. The paper examines the static fatigue behaviour of SiC-based Hi-Nicalon fibers at higher temperatures (≥ 900°C), when oxidation is enhanced. The influence of the oxide layer which grows at the surface of fiber is investigated. Fiber tows were subjected to static fatigue tests at 900°C and 1000°C. The slow crack growth based model which has been established earlier was revisited in order to introduce the contribution of oxide fiber coating. The model was found to describe satisfactorily the static fatigue behaviour of fiber tows at these high temperatures.

1. INTRODUCTION

Ceramic matrix composites (CMCs) are very attractive for structural applications at high temperatures. Nowadays, they are essentially used in space and defence applications. They are now considered for introduction in aircraft engines components. The control and prediction of CMC lifetime thus becomes a crucial issue.

Delayed failure of SiC/SiC composites, and SiC fibers has been observed under stresses far smaller than the stress to failure, essentially at temperatures below 800°C [1, 2], but also at higher temperature [3].

Previous work has also shown that the delayed failure of SiC-based fibers and tows was satisfactorily predicted by a slow crack growth based model, in the previously mentioned range of intermediate temperatures (< 800°C) [4]. The present paper focuses on higher temperatures (900°C and 1000°C), when additional effects related to oxidation rate and temperature are expected. The static fatigue behaviour of tows of SiC fibers (Hi-Nicalon, Nippon Carbon Co., Japan), has been investigated. The experimental data were analyzed using the subcritical crack growth model that has been proposed earlier for single fibers. The model has been revisited so as to account for oxidation related features. The model is based on the following crack velocity equation [4]:

$$V = A_1 K_I^n \qquad (1)$$

Where V is crack velocity, A_1 and n are constant and K_I is the stress intensity factor.

Under a constant stress σ, the lifetime of a single filament is the time required for the growth of the critical flaw, from initial size c_j to critical length a_c:

$$t = \int_{c_j}^{a_c} \frac{da}{V} \qquad (2)$$

Introducing fracture mechanics based crack size-stress relationships, and integrating equation (2) give:

$$t = \frac{2K_{IC}^{2-n}}{\sigma^n A_1 (n-2) Y^2}\left[\sigma_f^{n-2} - \sigma^{n-2}\right] \qquad (3)$$

With $A_1 = A_{10} \exp\left[-\frac{E_a}{RT}\right]$

K_{IC} is the critical stress intensity factor, Y is a crack shape factor, E_a is the activation energy, T is temperature, R= 8.314 J K^{-1} mol^{-1}, σ_f is the fiber strength in the absence of environmental effect.

Statistical distribution of fiber strengths is described satisfactorily by the conventional Weibull equation:

$$P = 1 - \exp\left[-\frac{V_f}{V_o}\left(\frac{\sigma_f}{\sigma_o}\right)^m\right] \qquad (4)$$

Where P is failure probability, V_f is the fiber volume, V_o is the reference volume, σ_o and m are statistical parameters.

2. EXPERIMENTAL PROCEDURE

A Hi-Nicalon tow contains 500 filaments of 15 µm average diameter each. During the static fatigue tests, the gauge length (25 mm) was located in the furnace hot-zone at a uniform temperature. It is defined as the distance between the grips (hot grip test method). A silica tube protected sample against possible pollution from furnace elements. This allowed environment control through a constant gas flow (N_2/O_2). The test specimens were heated up to the test temperature before loading (heating rate ~ 20°C/min). Then a dead-weight-load was hung slowly (this operation took < 10 s). Lifetime was captured automatically in the computer when specimen failed. Tow ends were affixed within alumina tubular grips using an alumina-based cement. Much care was taken during test specimen preparation and handling. A specific device for specimen preparation was used to ensure good alignment of tows and of filaments within the tows. For this purpose, a low load (12 g) was applied on tows.

Stress on multifilament tows was derived from the applied load, using the following equation which takes into account the individual fibre failures induced by the applied load:

$$\sigma = \frac{Fg\rho l N_0}{m_t\left[N_0 - N(F)\right]} \qquad (5)$$

where F is the applied load, g is gravity constant, ρ is tow density, l is the gauge length, and m_t is tow mass. N_o is the initial number of unbroken fibres and N(F) the number of fibres broken when applying the load F.

A few static fatigue tests were carried out using the cold grip technique, on much longer tows (gauge length = 300 mm). Temperature varied along the specimens, from the test temperature in the furnace to room temperature in the grips. Tow deformation was measured using a LVDT extensometer.

A few monotonic tensile tests were conducted at room temperature in order to determine the residual stress-strain behaviour after static fatigue. A standardized testing procedure was applied [5]. The tows were loaded at a constant deformation rate (5 mm/min). The tows were previously subjected to short term static fatigue using the hot grip technique: 20 mn heat up and cooling down and 15 mn at the test temperature, applied stress = 1.7 MPa, temperatures = 500°C, 800°C 900°C and 1000°C.

The fractured specimens were examined using scanning electron microscopy.

3. RESULTS AND DISCUSSION

3.1 Static fatigue under a constant temperature (hot grip technique)

Figure 1 shows plots of the rupture times that were measured under various constant loads. The stress-rupture time dependence is well fitted by the slow crack growth law that has been established at lower temperatures (500°C and 800°C) [4, 6]. As indicated in introduction, the law reduces to:

$$t\sigma^n = A_0 \exp\left[\frac{E_a}{RT}\right] \quad (6)$$

with $A_0 = 5.62\ 10^{17}\ s^{-1}\ MPa^{-n}$, n= 8.4 and $E_a = 181.6\ kJ\ mol^{-1}$ [6].

Equation (6) describes quite well the average stress-rupture time behaviour at 900°C and 1000°C. At 1000°C, the following features can be noticed:

- the scatter in rupture times at a given stress is much larger when comparing to data at 900°C,
- the stress at instantaneous fracture decreases tremendously as temperature increases.

Furthermore, comparison of data obtained at 900°C and 1000°C clearly indicates that a certain amount of specimens exhibited longer lifetimes at 1000°C.

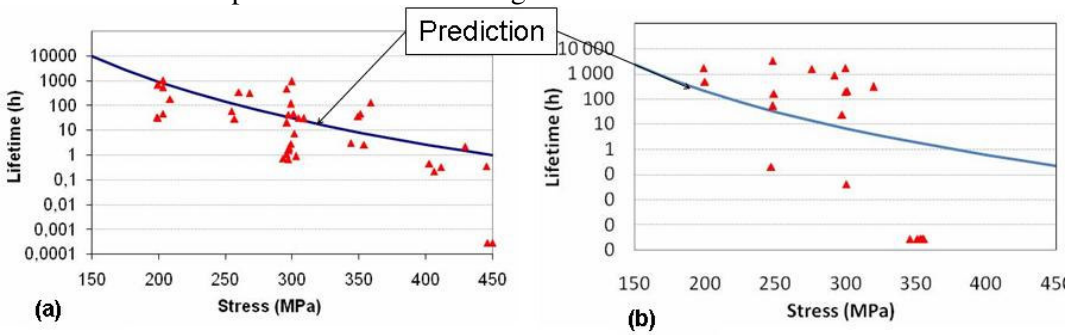

Figure 1: Stress rupture time data at 900°C (a) and 1000°C (b).

Figure 2 shows temperature dependence of tow instantaneous failure. It appears that this trend is at variance with that one observed on single filaments, which suggests the contribution of an extraneous effect involving the fiber framework. This weakening of tows can be logically attributed to fiber interactions [7]. Under the actual environment conditions that were applied to the tows, it seems reasonable to relate the interactions to fiber oxidation, since it is well known that an oxide layer forms at the surface of fibers, and that growth rate increases with temperature [8, 9].

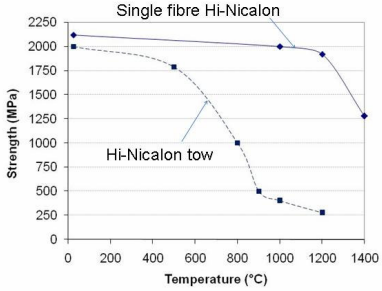

Figure 2: Temperature dependence of strength of tows and single Hi-Nicalon filaments.

3.2. Static fatigue in the presence of a temperature gradient (cold grip technique)

Figure 3 shows the location of fracture. It can be noticed that the tow failed from outside the furnace, where the temperature was around 600°C, whereas the portion of tow subjected to the test temperature of 1000°C survived. This result demonstrates that lifetime may be longer at 1000°C. This is consistent with the trend indicated by the stress rupture data at 1000°C versus those at 900°C (figure 1). Furthermore, it is worth pointing out that the part of the fibers that was exposed to 1000°C was coated by a thick layer of oxide. From Figure 3, it can be also noticed that tow deformations remained constant during the tests. This result demonstrates that creep did not occur at all the temperatures below 1000°C, under a stress of 200 MPa.

This result is consistent with previous results obtained on single SiC fibers for which creep was observed from 1200°C. It also suggests that the weakening of tows does not result from a degradation of the whole fiber which would cause a strain increase, or a stiffness decrease. It is in agreement with the presence of a local damage phenomenon such as slow growth of pre-existing flaws.

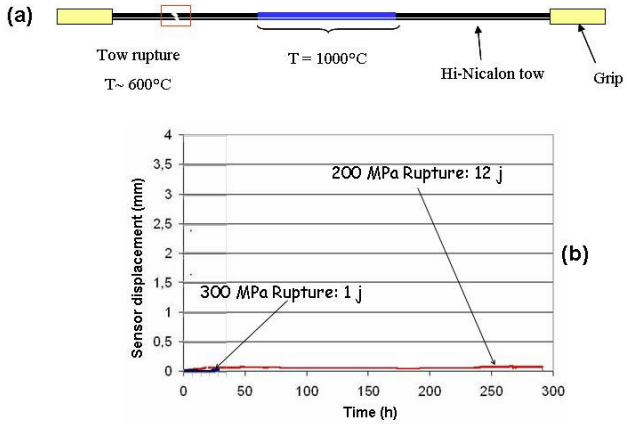

Figure 3: Static fatigue using the cold grip technique: (a) schematic diagram showing the specimen and failure location, (b) deformations of tows

3.3. Residual stress-strain behaviour

Figure 4 shows the stress-strain behaviour of tows that had been subjected to static fatigue at temperatures ranging from 500°C to 1000°C. It appears that the stress-strain behaviour is highly dependent on the test temperature.

After fatigue at 500°C, the stress-strain behaviour is identical to that one obtained with tows that have not experienced fatigue tests. The rupture stress is unchanged at 1800 MPa (maximum force = 130 N) and the stress-strain curves exhibit the typical downward curvature reflecting individual fiber breaks prior to ultimate failure [7].

After fatigue tests at higher temperatures, the stress-strain behaviour was tremendously affected.

- The failure stress was significantly smaller. It decreased from 1800 MPa to 500 MPa (35 N). The strength decrease was commensurate with the fatigue test temperature,
- The curve does not exhibit a continuous curvature, but instead load drops and linear segments, suggesting that groups of fibers failed.

From the load drops, the number of fibers which failed together can be determined [7]. Figure 4 shows that failures of groups of fibers produce the features that have been

displayed by the experimental curves. Table 1 reports the fractions of fibers which failed at each load drop. These fractions were estimated, using the following equation:

$$\frac{N_2}{N_1} = 1 - \frac{F_2}{F_1} \qquad (7)$$

where N_1 and N_2 are the numbers of surviving fibers corresponding to F_1 and F_2 respectively, at a given strain.

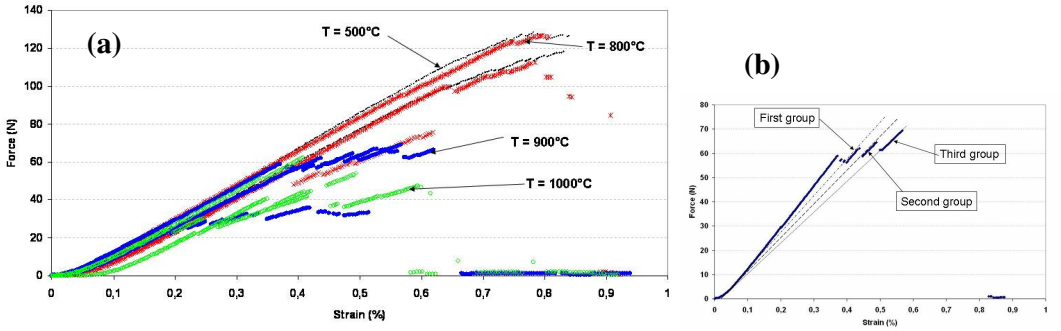

Figure 4: Force strain curves under monotonic tensile loading at room temperature on tows that experienced static fatigue at high temperatures during 15 minutes: (a) experimental results, (b) predictions

T°C	1st group	2nd	3rd	4th	5th	6th	7th
1000°C - 1	7	127	-	-	-	-	-
1000°C - 2	35	86	-	-	-	-	-
1000°C - 3	39	8	73	19	6	-	-
900°C - 1	49	31	29	-	-	-	-
900°C - 2	21	18	16	12	15	34	-
900°C - 3	23	23	31	14	19	40	28
800°C - 2	67	13	11	5	-	-	-
800°C - 3	31	-	-	-	-	-	-

Table 1: Groups of fiber failures during tensile residual tests, calculated using equation (7).

3.4. Fracture surfaces

Figures 5 and 6 show the typical fracture patterns with successive crack fronts that have been detected on Hi-Nicalon tows after static fatigue at 900°C and 1000°C. This demonstrates the presence of slow crack growth. It supports results reported above (figure 1). Figures 5 and 6 also show the presence of an oxide layer on the fibers. It is obvious from the micrographs that layer thickness is much more significant on those tows which experienced fatigue at 1000°C. It can also be noticed from figure 6 that some fibers were stuck by the oxide layer and from figure 7 that groups of fibers failed simultaneously.

Figure 8 provides evidence of groups of fibers which failed together during residual tests. It is worth pointing out that these tows were subject to short static fatigue (15 minutes).

Thus, microscopy supports the analysis of experimental results.

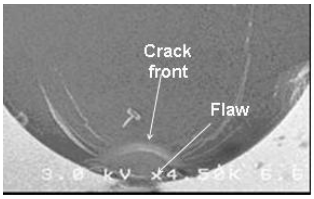

Figure 5: SEM micrograph showing the fracture surface of a Hi-Nicalon fiber after static fatigue on a tow at 900°C, under a stress of 250 MPa during 14 days.

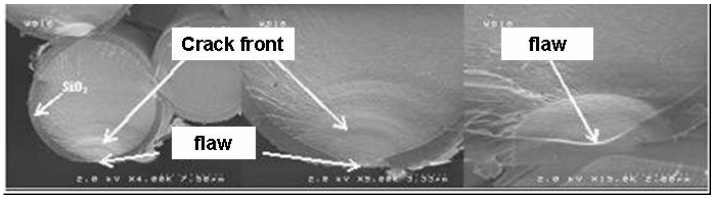

Figure 6: SEM micrograph showing fracture surfaces of fibers in a Hi-Nicalon tow after static fatigue at 1000°C, under a stress of 250 MPa during 13 days.

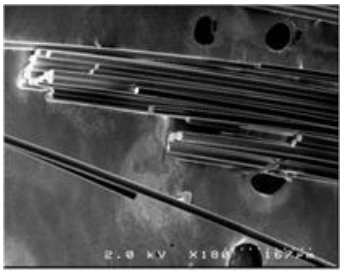

Figure 7: Micrograph showing a group of fiber failures after static fatigue at 1000°C, under a stress of 250 MPa during 13 days.

Figure 8: SEM micrograph showing fracture surfaces of fibers after tensile test at room temperature on a tow which had been subjected to static fatigue at 1000°C for 15 mn

4. PREDICTION OF STRESS-STRAIN TIME CURVES

The model of static fatigue of fibers has been revisited in order to take into account the effects of oxide fiber coating at temperatures above 900°C, i.e. the increase in lifetime and the increase in variability.

The increase in lifetime can be logically attributed to protection by the oxide layer which caused a decrease in the oxidation rate. It was treated by introducing slowing down of crack extension, through constant A_1 which determines constant A, as demonstrated in a previous paper [6]. For this purpose, a time dependent retardation function was used, according to [11], so that A takes the following form:

$$A = A_0 \exp\left[\frac{E_a}{RT} + f(t_0)\right] \qquad (8)$$

$f(t_0)$ operates when the oxide layer at the surface of fiber reaches a critical thickness at t_0:

$$f(t_0) = f.H\,(t-t_0) \qquad (9)$$

with H = 0 when $t < t_0$, and H = 1 when $t \geq t_0$; $t_0 = \frac{d_{oxide}^2}{kT}$; f is a constant. f was set to 3.

with d_{oxide} is the critical thickness of the oxide layer:

$k = 1.07\ 10^{-11} \exp\left[\frac{20326}{T}\right]$ when T < 1000°C [12]

$k = 2.5\ 10^{-19} \exp\left[\frac{91000}{RT}\right] P_{02}^{0.89}$ when T = 1000°C [12]

It was considered that, at critical time t_0, grain boundaries have been completely filled by oxide:

$$d_{oxide} = d_f + \frac{1}{2} d_{gb} \qquad (10)$$

where d_f is the thickness of outer fiber surface which has been consumed, and d_{gb} is the width of grain boundaries. d_{gb} was measured by image analysis of SEM micrographs: d_{gb} = 40 nm. d_f was estimated from the stoichiometric equation of SiC fiber oxidation. d_{oxide} was estimated to be 50 nm, from equations (10). Table 2 summarizes the values of k and t_0.

Figure 9 shows the crack velocity decrease predicted using the retardation function. Figure 10 shows that the upper rupture times were satisfactorily described by the model. Fiber characteristics introduced into stress-rupture time equations are summarized in table 3.

	k(s.m^{-2})	**to (s)**
500°C	4,08.10^{-24}	612927268
800°C	6,4.10^{-21}	393152
900°C	3,2.10^{-20}	78200
1000°C	3,1.10^{-19}	8057

Table 2: Values of constant k and critical time t_o.

	900°C	**1000°C**
A_0 (s^{-1} MPa^{-n})	5,62 E+17	5,62 E+17
E_a (J/mol)	181600	181600
R (J/mol/K)	8,314	8,314
Y	1,13	1,13
K_{IC} (MPa. √m)	1,25	1,25
$\sigma_{r\ min}$ (MPa)	350	350
$\sigma_{r\ max}$ (MPa)	1790	1790
$\sigma_{r\ moy}$ (MPa)	1100	1100
V (m^3)	3,56 E-12	3,56 E-12
A_1 (MPa^{-n} s^{-1} $m^{1-n/2}$)	1,54 E-08	6,66 E-08
f	3	3
k (m^2/s)	3,10 E-19	3,20 E-20
n	8,4	8,4
Critical silica layer (m)	5,00 E-08	5,00 E-08

Table 3: Fiber characteristics that were used for stress-rupture time predictions.

It was considered that variability is related to the fiber interactions caused by the presence of an oxide layer at the surface of fibers. As shown by figure 2, the strength of tows is comprised between a temperature dependent minimum value and a maximum value corresponding to the reference tow strength at room temperature:

$\sigma_{r\ min}$ (T) ≤ σ_r ≤ $\sigma_{r\ max}$ (1800 MPa)

Therefore, lower and upper bounds for stress-rupture time data were obtained by inserting $\sigma_f = \sigma_{min}$ (T) and $\sigma_f = \sigma_{max}$ (1800 MPa) into equation (3) (table 3).

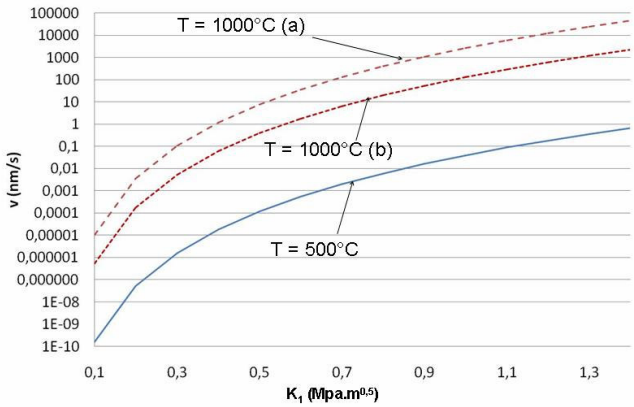

Figure 9: Crack velocity diagram at various temperatures, predicted using the slow crack growth equation $V=A_1K_I^n$ for Hi-Nicalon fibers (a) at 1000°C when $t < t_0$ and (b) at 1000°C when $t \geq t_0$.

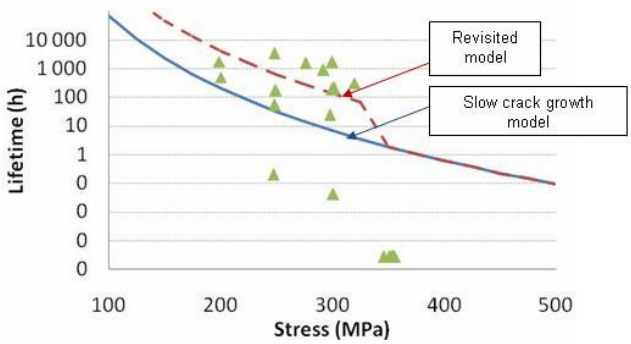

Figure 10: Stress-rupture time diagram predicted using the slow crack growth model and the model revisited.

5. CONCLUSIONS

Results of experiments and SEM fractography and the slow crack growth based model lead to the same conclusions. At 900°C and 1000°C, delayed failure of tows is caused by a slow crack phenomenon, as observed earlier at lower temperatures. As temperature increases, the fibers are coated by a thicker oxide layer, which influences the slow crack growth phenomenon. The crack velocity slows down, and fiber interactions are enhanced, which leads to longer lifetimes under low stresses and smaller stresses at instantaneous failure. The oxide coating associated effects were introduced into the slow crack growth based model. The lifetimes that were calculated were found in excellent agreement with experimental results. In particular, variability associated to fiber interactions was satisfactorily described. Finally, it is worth pointing out that tests using the cold grip technique showed that deformations remained constant at temperatures below 1000°C. This demonstrates that creep did not occur at these temperatures and that the phenomena involved do not affect the whole fiber, which is consistent with slow crack growth.

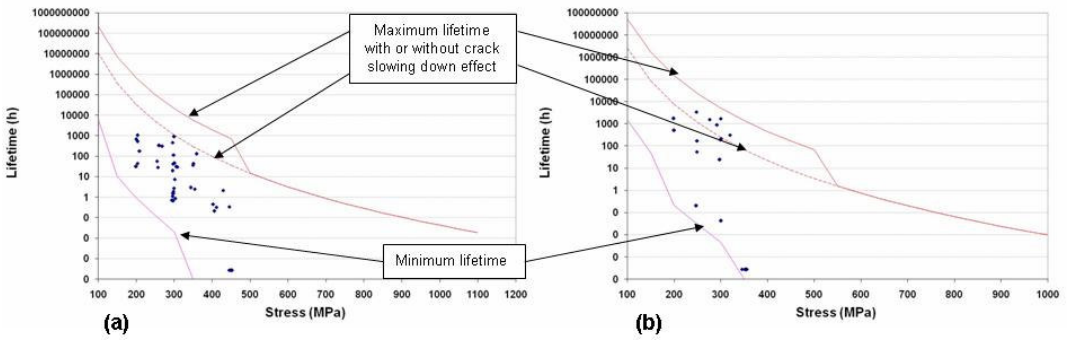

Figure 11: Predictions of scatter in stress-rupture time data.

ACKNOWLEDGEMENTS

The support of CNRS, SNECMA PROPULSION SOLIDE and DGA is highly appreciated. The work was carried out within the frame of a CPR program entitled "Modelling, prediction and validation of CMC lifetime" and involving the following laboratories: INSA Lyon, LMT Cachan, PROMES Perpignan, CEAT Toulouse.
The authors are indebted to Mrs. J. Forget for help in preparation of manuscript.

REFERENCES

1- Bertrand S., Pailler R., and Lamon J., "Influence of strong fiber/coating interfaces on the mechanical behaviour and lifetime of Hi-Nicalon/$(PyC/SiC)_n$/SiC minicomposites", *J. Am. Ceram. Soc*., 2001;84,4:787-94.
2- Forio P., Lavaire F and Lamon J., "Delayed failure at intermediate temperatures (600°-700°C) in air in silicon carbide multifilament tows", *J. Am. Ceram. Soc*., 2004;87,5:888-893.
3- Lara-Curzio E., "Stress-rupture of Nicalon/SiC continuous fiber ceramic composites in air at 950°C", *J. Am. Ceram. Soc*., 1997;80,12:3268-72.
4- Gauthier W., Lamon J., "Delayed failure of silicon carbide fibers in static fatigue at intermediate temperatures (500-800°C) in air", *Ceram. Engineering and Science Proceedings*, Volume 28, Issue 2, edited by Edgar Lara-Curzio, John Wiley & Sons, Inc., USA, 423-431,2008.
5- European Standard, Advanced technical ceramics – Ceramic Composites – Method of test for reinforcement – Part 5 : Determination of distribution of tensile strength and of tensile strain-to-failure of filaments within a multifilament tow at ambient temperature, ENV 1007-5, 1998.
6- Gauthier W., Lamon J., "Delayed failure of Hi-Nicalon and Hi-Nicalon S multifilament tows and single filaments at intermediate temperatures (500-800°C)" *J. Am. Ceram. Soc*., to be published.
7- Calard V., Lamon J., "Failure of fiber bundles", *Composites Science and Technology*, 2004,64:701-710.
8- Gogotsi Y., Yoshimura M., "Oxidation and properties degradation of SiC fibers below 850°C", *J. Materials Science Letters*, 2004,13:680-683.
9- Shimoo T., Kakehi Y., Kakimoto K. and Kamura K.O., *J. Japan Inst. Metals*, 1992,56:175.
10- Lara-Curzio E., "Oxidation induced stress-rupture of fiber bundles", *J. Engineering Materials and Technology*, 1998,120:105-109.

11- S.M. Wiederhorn, “Influence of water vapor on crack propagation in Soda-lime glass”, *Journal of the American Ceramic Society*, 1967, 50:407–414.
12- Avril L., Rebillat F., Legallet S., Louchet C., Guette A., “Quantitative approach to oxidation of Hi-Nicalon SiC fibers”, presented during “Journées du Groupe Français des Céramiques”, 2005, Paris.